Solvated excess protons in water: quantum effects on the hydration structure

Solvated excess protons in water: quantum effects on the hydration structure

Dominik Marx†, Mark E Tuckerman‡ and Michele Parrinello†

† Max-Planck-Institut für Festkörperforschung, Heisenbergstrasse 1, 70569 Stuttgart, Germany
‡ Department of Chemistry and Courant Institute of Mathematical Sciences, New York
University, 4 Washington Place, New York, NY 10003, USA

Abstract. The hydration of one excess proton in water under ambient conditions is investigated by means of atomistic computer simulations. The *ab initio* path integral technique employed takes into account nuclear quantum effects such as tunnelling and zero-point motion at finite temperatures. In addition, the interactions are calculated by 'on-the-fly' electronic structure calculations in the framework of density functional theory.

(Some figures in this article appear in black and white in the printed version.)

1. Grotthuss diffusion and fluctuations

The idea of 'structural diffusion' of protons in water was introduced by von Grotthuss nearly two hundred years ago. The basic idea is that it is not an individual proton (nor a rigid hydrated complex $H^+ \bullet (H_2O)_n$) that undergoes hydrodynamic Stokes or vehicle diffusion, but rather a structural charge defect in the tetrahedral hydrogen-bonded water network [1]. This is possible since the strong covalent O–H bonds (which hold together the individual water molecules) and the weak hydrogen O$\cdots$H bonds (which connect the water molecules to a tetrahedral network) can be fairly easily interconverted: $O_a–H^\star \cdots O_b \rightarrow O_a \cdots H^\star–O_b$ by moving the shared proton from one water molecule to a neighbouring one. Although every textbook on physical chemistry contains a discussion and an 'explanation' of the anomalously fast diffusion of protons in acids based on that caricature, 'the actual mechanism is still highly contentious' [1]. Among the controversial issues are those revolving around the nature of the hydrated proton and the influence of quantum versus thermal fluctuations. In a recent letter [2], it was revealed that the two complexes $H_5O_2^+$ and $H_9O_4^+$, which were previously discussed as *alternative* hydration structures [3,4], occur only in the sense of 'limiting' or 'ideal' structures.

In this communication, the extent to which quantum-mechanical effects are important in addition to the classical thermal fluctuations is addressed; the latter were already analysed in detail in the framework of *ab initio* molecular dynamics [5]. This debate has its roots in invoking different approximations in order to describe proton diffusion. Hückel was the first to introduce such a theory [6]: a H_3O^+ complex was modelled as a dipolar sphere which undergoes Debye-like relaxation in a structureless dielectric continuum. According to this model, proton transfer is driven by thermally activated and spatially isotropic proton jumps from one water molecule to the next. The classical approximation was also advocated by Stearn and Eyring [7], this time in the framework of classical transition state theory. Another view was taken in the

independent papers by Bernal and Fowler [8] and Wannier [9]. In their models, quantum tunnelling in 'favourable configurations' is supposed to be the basic transfer mechanism, which in turn is *intrinsically* temperature *independent*. A different line of thought was initiated by Huggins who observed that the proton-transfer barrier of a hydrogen-bonded proton simply *vanishes* for small O_a–O_b distances [10]. This leads to the concept of adiabatic proton transfer [11] due to thermally induced barrier suppression with the result that the proton can transfer *without* crossing a barrier. Later theoretical studies are basically extensions, refinements, and combinations of these basic ideas. For instance Gierer and Wirtz [12] postulated a classically activated process, which is however strongly affected by the temperature dependence of the hydrogen-bond formation and breaking processes around the defect. With the advent of atomistic computer simulations, proton hydration and diffusion became the focus of various studies as documented by the extensive, although by no means exhaustive list of references [17–31, 38] given in reference [2]. A review of pertinent experimental data is provided in reference [13].

2. Technicalities

The *ab initio* path integral technique [14] is used where both the electrons and nuclei are treated as quantum particles; for reviews see reference [15]. The periodic cubic simulation box with a linear dimension of 9.8652 Å contains 32 oxygen and 65 hydrogen atoms, which corresponds to adding one excess proton to 32 water molecules. The *ab initio* interactions are calculated 'on the fly' within Hohenberg–Kohn–Sham density functional theory using the BLYP functional, Troullier–Martins pseudopotentials, and a Γ-point plane-wave expansion of the valence orbitals up to 70 Ryd; see reference [2]. The quantum as well as a classical reference simulations were performed in the canonical ensemble, both at 300 K, and the Feynman path integral in the former case was discretized using $s = 1, \ldots, P = 8$ Trotter slices whereas the classical limit is obtained for $P = 1$.

3. Dissecting the quantum effects

In order to investigate the structure of the migrating structural defect, a criterion based on the asymmetric stretch coordinate $\delta = R_{O_aH^\star} - R_{O_bH^\star}$ of the shared proton $H^\star$ in the hydrogen-bonded atom triple $O_aH^\star O_b$ is introduced [2]. The definition of one $H_3O_a^+$ unit by assigning every proton to its closest oxygen atom (separately for each Trotter slice) turned out to be unambiguous in most cases, and O_b and $H^\star$ are those oxygen and hydrogen atoms that form together with O_a the shortest δ-coordinate in this particular configuration. This $O_aH^\star O_b$ triple is what is called the 'most active hydrogen bond' and $H^\star$ is the 'special proton'. Here we analyse the structure of the defect [16] in the limit of 'small' and 'large' $|\delta|$ in figures 1(a) and 1(b), respectively. The radial distribution functions for small $|\delta|$ are consistent with an $H_2O\cdots H^+\cdots OH_2$ or $H_5O_2^+$ complex, in which a proton is equally shared between two normal water molecules H_2O_a and O_bH_2. In such situations, the proton in the most active hydrogen bond is located 'symmetrically' between two water molecules, forming with both of them short/strong hydrogen bonds. For large $|\delta|$, the configurations correspond to a $H_3O^+\bullet (H_2O)_3$ or $H_9O_4^+$ complex, where the H_3O^+ core is roughly threefold coordinated by normal water molecules. In this limit, the proton in the most active hydrogen bond can nevertheless be defined. It is found to be preferentially attached 'asymmetrically' to one water molecule via a strong covalent bond, thus forming the $H_3O_a^+$ core, and donates a hydrogen bond to the water molecule H_2O_b in its first solvation shell. Nuclear quantum effects (thick lines) seem to affect the *structure* of both defects only to a negligible extent by *slightly* broadening the peaks; cf. the
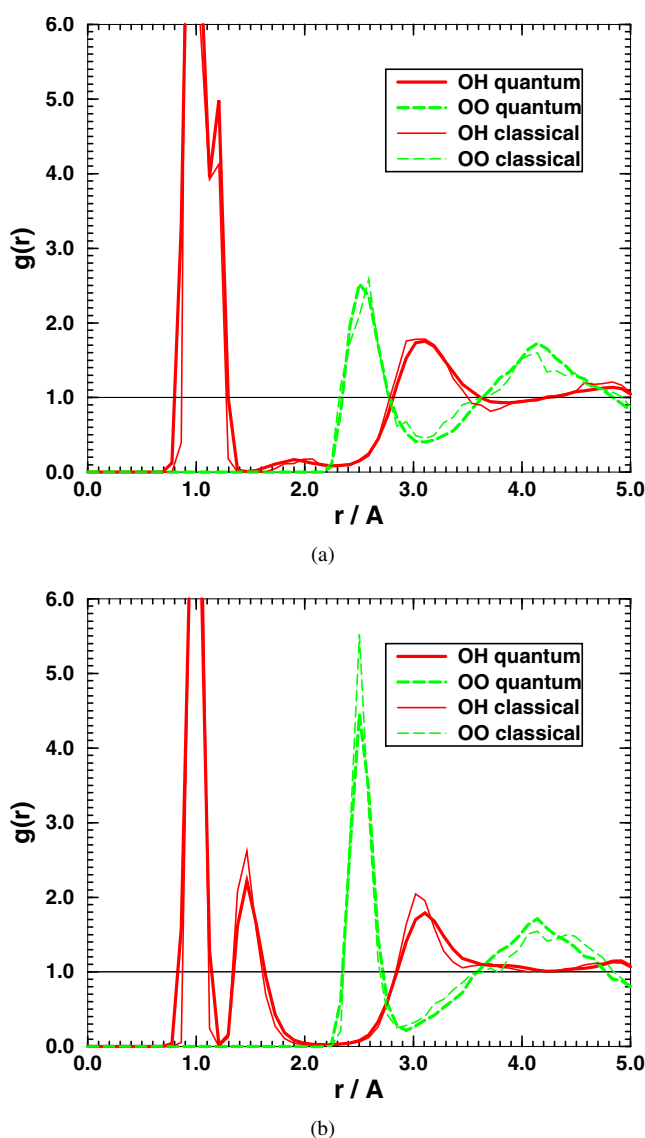
Figure 1. Partial radial distribution functions $g_{XY}(r)$ for $H_5O_2^+$ (a) and $H_9O_4^+$ (b) complexes for oxygen–hydrogen (solid lines) and oxygen–oxygen (dashed lines) XY pairs, where the thick and thin lines distinguish simulations with quantum and classical nuclei, respectively. For $H_5O_2^+$: only those XY pairs where at least one of the two atoms belongs to the $O_aH^\star O_b$ triple with $|\delta| \leqslant 0.1$ Å are included. For $H_9O_4^+$: only those XY pairs where at least one of the two atoms belongs to the $H_3O_a^+$ core and $|\delta| > 0.3$ Å are included.

thin lines in figure 1 stemming from the reference simulation with classical point particles as nuclei. Does this mean that quantum fluctuations are totally irrelevant in the discussion of proton diffusion in water at ambient conditions?

To this end, the free-energy profile [15] (or potential of mean force) for proton transfer along the most active hydrogen bond $O_a–H^\star\cdots O_b \rightleftharpoons O_a\cdots H^\star–O_b$ is computed separately for the quantum and classical cases; see figure 2. Classically, the symmetric $H_5O_2^+$-like defects,
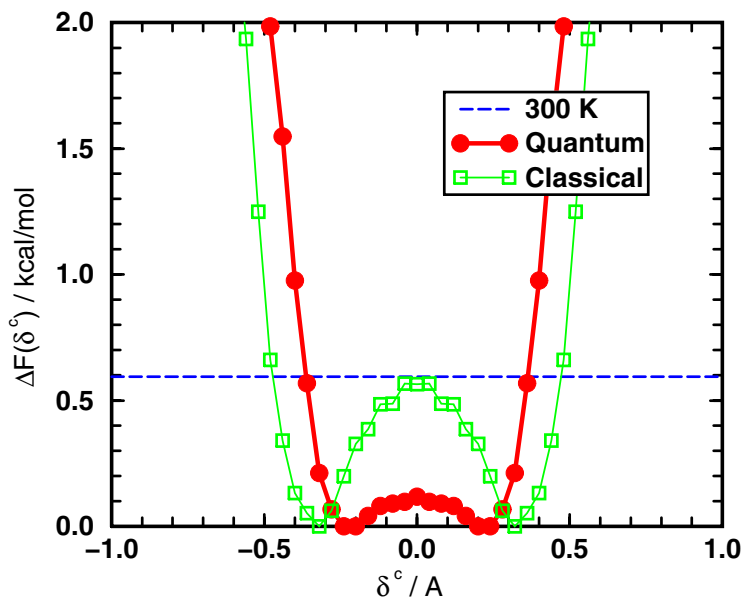
Figure 2. The proton-transfer free-energy profile $\Delta F(\delta)$ from quantum (circles, thick line) and classical (squares, thin line) simulations both at 300 K; the horizontal dashed line marks $k_B T$ at 300 K $\approx$ 0.59 kcal mol^{-1} and the functions are symmetrized around $\delta = 0$ Å. In the quantum case the necessary path centroid coordinate $\delta^c = \sum_{s=1}^{P} \delta^{(s)}/P$ is computed by locating the $O_aH^\star O_b$ triple in every Trotter slice $s = 1, \ldots, P$ separately, from which $\delta^{(s)}$ is determined.

characterized by $|\delta| \approx 0$ Å, are unstable by about 0.6 kcal mol^{-1} relative to the minima of the free energy, which occur at $\delta \approx \pm 0.3$ Å, i.e. for the asymmetric $H_9O_4^+$-like complexes. This situation changes *qualitatively* upon including quantum fluctuations: the barrier is suppressed down to a fraction of the thermal energy at 300 K. Thus, proton transfer *within* the most active hydrogen bond is an essentially barrierless rattling motion of the special proton $H^\star$ in a very flat potential of mean force due to zero-point energy. This implies that the $H_5O_2^+$ and $H_9O_4^+$ limiting structures of the defects are constantly interconverted into each other. Thus, the most active hydrogen bond can be categorized as a so-called 'low-barrier hydrogen bond' [17] where the zero-point energy is close to the *classical free-energy* barrier.

A tool for analysing 'microscopically' nuclear wave packets in path integral simulations is provided by r.m.s. position–displacement correlation functions of the Feynman paths:

$$\mathcal{R}(s) = \left\langle \left| Q^{(1)} - Q^{(s)} \right|^2 \right\rangle^{1/2} \qquad \text{with} \qquad s = 1, \ldots, P+1 \qquad \text{and} \qquad Q^{(1)} \equiv Q^{(P+1)}$$

which measure the correlation between different Trotter slices of some (generalized) coordinate $Q^{(s)} = Q(\{R_I\}^{(s)})$, where $R_I^{(s)}$ is the cartesian coordinate of the Ith nucleus in Trotter slice s and $\langle \cdots \rangle$ denotes the canonical configurational average; note that $\mathcal{R}(s) \equiv 0$ in the classical limit. For a *free* particle, the value at the maximum, $\mathcal{R}(s = P/2)$, is equal to the thermal de Broglie wavelength or equivalently to the spread of the associated Gaussian wave packet (within trivial numerical constants), so $\mathcal{R}(P/2)$ is taken as a measure of the particle's extent also in the interacting case. Averaging over all 65 protons in the sample (using $Q^{(s)} = R_{H_I}^{(s)}$) leads to a behaviour quite similar to that of free protons at the same temperature; see figure 3. This changes drastically if the position of the special proton $H^\star$ used as a 'marker' of the structural defect is autocorrelated (where $Q^{(s)} = R_{H^\star}^{(s)}$; note that the identity I of $H^\star$ might
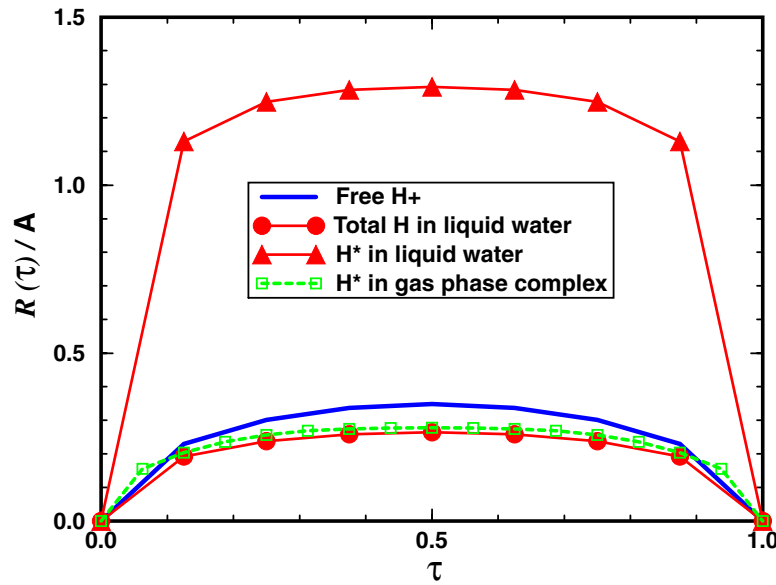
Figure 3. The position correlation function $\mathcal{R}(\tau)$ at 300 K for a free proton (solid line), the average of all 65 protons (circles), the special proton H* (triangles), and for comparison the shared proton H* in the hydrogen bond of an *isolated* $H_5O_2^+$ complex in the gas phase (based on reference [17] where $P = 16$; the corresponding average including all five protons of the complex is identical within the statistical error); here $\tau = (s - 1)/P \in [0, 1]$ with $s = 1, \ldots, P + 1$ ($\equiv 1$).

change along Feynman paths $s = 1, \ldots, P$). The associated wave packet acquires about five times the spread of the average proton! Since a particular (labelled) proton cannot spread out that much, the large spread reflects the quantum delocalization of the *structural defect* (which is not necessarily associated with a particular proton I) over more than one hydrogen bond. This interpretation is supported by the observation that the correlation function calculated for all protons and separately for H* in an *isolated* $H_5O_2^+$ complex in the *gas phase* [17], where there is *one* hydrogen bond and thus only *one particular* shared proton H*, leads to values very similar to that of the average proton in the liquid; see figure 3.

The average 'size' of the defect itself, corresponding to the spread of the associated wave packet, can be quantified by the radius of gyration of the H_3O^+ subunit:

$$R^{\mathrm{gyr}} = \left\langle \frac{1}{N} \sum_{I=1}^{N} \frac{1}{P} \sum_{s=1}^{P} (\boldsymbol{R}_I^{(s)} - \boldsymbol{R}^{\mathrm{c}})^2 \right\rangle^{1/2} \qquad \text{with} \qquad \boldsymbol{R}^{\mathrm{c}} = \frac{1}{N} \sum_{I=1}^{N} \frac{1}{P} \sum_{s=1}^{P} \boldsymbol{R}_I^{(s)}$$

where I labels the $N = 4$ atoms in the tagged $H_3O_a^+$ subunit as determined separately in every Trotter slice s and thus might also change labels along the Feynman paths. It amounts to roughly 0.9 Å for an isolated H_3O^+ molecular ion in the gas phase. The classical distribution functions in figure 4, which already include thermal fluctuations at 300 K, are close to the gas-phase value in both complexation environments $H_5O_2^+$ and $H_9O_4^+$ as distinguished by the above-mentioned δ-criterion. Additional quantum fluctuations lead to a significant increase of the size of the H_3O^+ subunit. Interestingly, the two environments lead to different behaviours: the H_3O^+ subunit is largely delocalized (between two *or more* water molecules) in the $H_5O_2^+$ environment, whereas, in $H_9O_4^+$ complexes, it is preferentially localized (trapped at a *particular* water molecule) similarly to the classical limit; note that these effects are again linked to quantum effects concerning the structural defect rather than those related to particular atoms.

(a)

(b)
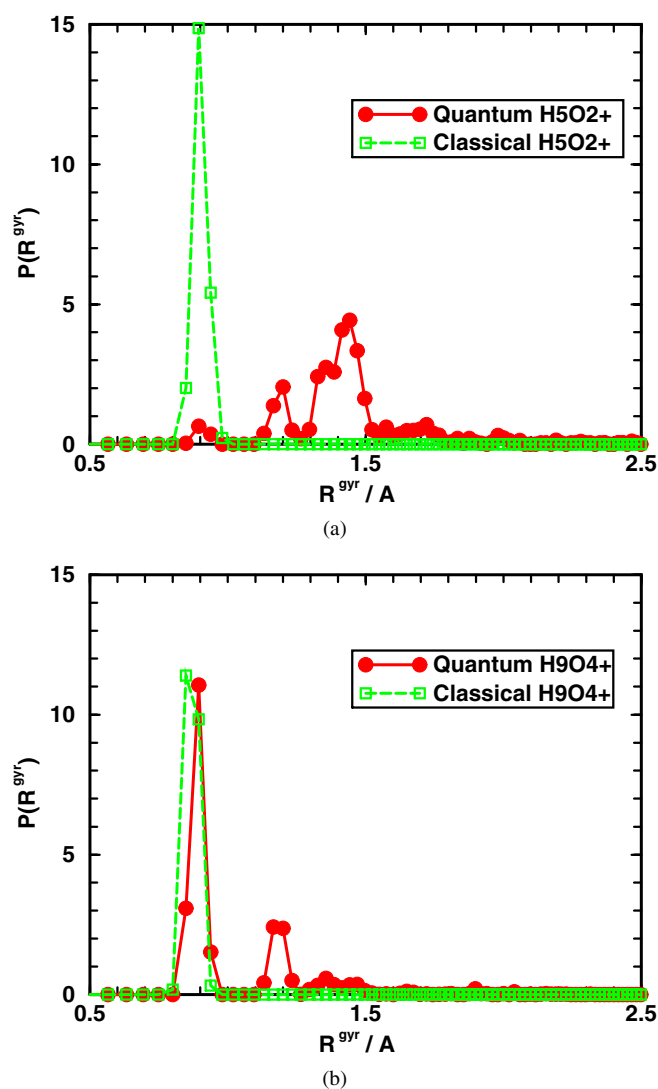
Figure 4. The radius-of-gyration distribution function $P(R^{gyr})$ for the H_3O^+ subunit in the complexes $H_5O_2^+$ where $|\delta| \leqslant 0.1$ Å (a) and $H_9O_4^+$ where $|\delta| > 0.3$ Å (b) from quantum (circles, solid line) and classical (squares, dashed line) simulations.

4. Future perspectives

Although many insights into the mechanism of proton diffusion have already been gained with state-of-the-art computer simulation techniques, the vast area of proton transfer along hydrogen bonds will remain an active field of research for quite a few years to come. In particular, the aim will be to develop methods that allow study of the real-time quantum dynamics of large many-body systems within the *ab initio* framework without the introduction of simplifying models. A first step in this direction was undertaken recently [18].

References

[1] Atkins P W 1998 *Physical Chemistry* 6th edn (Oxford: Oxford University Press) ch 24.8, p 741
[2] Marx D, Tuckerman M E, Hutter J and Parrinello M 1999 *Nature* **397** 601
   See also
   Hynes J T 1999 *Nature* **397** 565
[3] Wicke E, Eigen M and Ackermann Th 1954 *Z. Phys. Chem., NF* **1** 340
[4] Zundel G and Metzger H 1968 *Z. Phys. Chem., NF* **58** 225
[5] Tuckerman M, Laasonen K, Sprik M and Parrinello M 1994 *J. Phys.: Condens. Matter* **6** A93
   Tuckerman M, Laasonen K, Sprik M and Parrinello M 1995 *J. Phys. Chem.* **99** 5749
   Tuckerman M, Laasonen K, Sprik M and Parrinello M 1995 *J. Chem. Phys.* **103** 150
[6] Hückel E 1928 *Z. Elektrochem.* **34** 546
[7] Stearn A E and Eyring J 1937 *J. Chem. Phys.* **5** 113
[8] Bernal J D and Fowler R H 1933 *J. Chem. Phys.* **1** 515
[9] Wannier G 1935 *Ann. Phys., Lpz.* **24** 545
[10] Huggins M L 1936 *J. Phys. Chem.* **40** 723
[11] Ando K and Hynes J T 1997 *J. Phys. Chem.* B **101** 10 464
[12] Gierer A and Wirtz K 1949 *Ann. Phys., Lpz.* **6** 257
[13] Agmon N 1995 *Chem. Phys. Lett.* **244** 456
   Agmon N 1996 *J. Chim. Phys. Phys.–Chim. Biol.* **93** 1714
[14] Marx D and Parrinello M 1994 *Z. Phys.* B **95** 143
   Marx D and Parrinello M 1996 *J. Chem. Phys.* **104** 4077
   Tuckerman M E, Marx D, Klein M L and Parrinello M 1996 *J. Chem. Phys.* **104** 5579
[15] Marx D 1998 *Classical and Quantum Dynamics in Condensed Phase Simulations* ed B J Berne, G Ciccotti
   and D F Coker (Singapore: World Scientific) p 359
   Marx D 1999 *New Approaches to Problems in Liquid State Theory* ed C Caccamo, J-P Hansen and G Stell
   (Dordrecht: Kluwer) p 439
[16] For small $|\delta| \leqslant 0.1$ Å, the first peak of the intracomplex $g_{OO}(r)$ occurs at $r \approx 2.4$ Å (compared to 2.8 Å
   for bulk water). The first peak of $g_{OH}(r)$ is at around 0.95 Å (close to the value found for bulk water); a
   secondary peak occurs close to 1.25 Å, (roughly half of the average O–O distance); however, no clearly
   distinguishable feature exists at $r \approx 1.8$ Å (where the first intermolecular peak for bulk water would be
   expected).
   For large $|\delta| > 0.3$ Å, $g_{OO}(r)$ peaks near 2.5 Å and the first peak of $g_{OH}(r)$ is close to 1.0 Å (which is slightly
   longer than for H_2O molecules in the bulk and consistent with a H_3O^+ molecule in the core). The H_3O^+
   core is roughly threefold coordinated whereas the surrounding first-shell H_2O molecules are approximately
   fourfold coordinated (similarly to the case for bulk water).
[17] Tuckerman M E, Marx D, Klein M L and Parrinello M 1997 *Science* **275** 817
[18] Marx D, Tuckerman M E and Martyna G J 1999 *Comput. Phys. Commun.* **118** 166